Eur Biophys J (2008) 37:783–792
DOI 10.1007/s00249-008-0270-7

ORIGINAL PAPER

Pressure induces interdigitation differently in DPPC and DPPG

Harpreet Singh · Jason Emberley · Michael R. Morrow

Received: 13 August 2007 / Revised: 16 January 2008 / Accepted: 17 January 2008 / Published online: 5 February 2008

Abstract The phase behaviours of chain-perdeuterated dipalmitoylphosphatidylcholine (DPPC-d_{62}) and chain-perdeuterated dipalmitoylphosphatidylglycerol (DPPG-d_{62}) bilayers were compared using ^{2}H nuclear magnetic resonance spectroscopy and quadrupole echo decay measurements over pressures ranging from ambient to 196 MPa and temperatures ranging from 60 to −25°C. At ambient pressure, the phase behaviours of DPPC-d_{62} and DPPG-d_{62} were nearly identical. At 196 MPa, their behaviours were also very similar and both lipids appeared to pass from an interdigitated gel phase at high temperature, through a non-interdigitated gel phase at intermediate temperature, to a chain-immobilized ordered phase at low temperature. At 85 MPa, the behaviour of DPPC-d_{62} was similar to its ambient pressure behaviour with no evidence of interdigitation. For DPPG-d_{62}, however, the behaviour at 85 MPa was similar to its higher pressure behaviour and spectra characteristic of an interdigitated gel phase were observed. Pressure-temperature phase diagrams for both lipids were compared. While the minimum pressure for DPPC-d_{62} interdigitation is about 150 MPa, DPPG-d_{62} was observed to interdigitate at pressures as low as 60 MPa. Given the similarity of their phase behaviours at both higher and lower pressures, this difference reflects the extent to which bilayer phase behaviour depends on the balance between interactions in the headgroup and hydrocarbon regions of the bilayer.

H. Singh · J. Emberley · M. R. Morrow (✉)
Department of Physics and Physical Oceanography,
Memorial University of Newfoundland,
A1B 3X7 St. John's, NF, Canada
e-mail: mmorrow@mun.ca

Keywords Phospholipids bilayer · High pressure · Phase diagram · Interdigitation · Deuterium NMR

Abbreviations

DPPC	1,2-dipalmitoyl-*sn*-glycero-3-phosphocholine
DPPG	1,2-dipalmitoyl-*sn*-glycero-3-phosphoglycerol
DPPC-d_{62}	1,2-perdeuterodipalmitoyl-*sn*-glycero-3-phosphocholine
DPPG-d_{62}	1,2-perdeuterodipalmitoyl-*sn*-glycero-3-phosphoglycerol

Introduction

The physical properties of phospholipid bilayers and membranes are determined by a variety of interactions between system components. Information about these interactions gained from studies of how phospholipid bilayers respond to changes in hydrostatic pressure complements and extends what is learned from studies at ambient pressure. Within the liquid crystalline phase, increasing pressure increases average chain order and so that the bilayer response to pressure is anisotropic (Braganza and Worcester 1986a, b; Driscoll et al. 1991a; Bonev and Morrow 1997b). Pressure also raises the main transition temperature of phospholipids bilayers and can induce transitions to ordered phases that are not accessible at ambient pressure. For single-component bilayers, the sensitivity of bilayer properties to pressure varies with chain length, degree of chain unsaturation, and headgroup. In mixed bilayers, pressure can both amplify and reduce differences between components.

Pressure–temperature phase diagrams for bilayers of dipalmitoylphosphatidyl-choline (DPPC) have been

determined using a variety of techniques including neutron-scattering (Braganza and Worcester 1986a; Winter and Pilgrim 1989), vibrational spectroscopy (Wong et al. 1988), ^{2}H NMR (Driscoll et al. 1991b), optical transmission (Kaneshina et al. 1992; Maruyama et al. 1997), volumetric measurements (Böttner et al. 1994) and synchrotron X-ray diffraction (Czeslik et al. 1998). In the DPPC phase diagram reported by Braganza and Worcester (1986a, b), the temperature for the main transition between the DPPC liquid crystalline or L_α bilayer phase and the more ordered gel phase increases with pressure at 0.23°C/MPa. A curved boundary separates a region of interdigitated gel at high pressure from the liquid crystalline phase at higher temperature and lower pressure and from the non-interdigitated gel at lower temperature and lower pressure. The minimum pressure on the interdigitated gel boundary, about 150 MPa, occurs at about 60°C. A similar minimum pressure for DPPC interdigitation was reported from neutron scattering results (Winter and Pilgrim 1989). Other studies have suggested minimum interdigitation pressures for DPPC as low as 100 MPa (Driscoll et al. 1991b; Maruyama et al. 1997). In this work, we follow the convention of labelling the interdigitated gel phase as $L_{\beta\mathrm{I}}$ (Winter and Pilgrim 1989).

In addition to $L_{\beta\mathrm{I}}$, the ambient pressure rippled gel phase $P_{\beta'}$ and the ambient-pressure planar gel phase $L_{\beta'}$, Wong et al. (1988) identified three additional high pressure ordered phases, GIII, GIV, and GV, using vibrational spectroscopy. Depending on how pressure and temperature is varied, transitions between the high-pressure ordered phases can be slow and the some of the ordered phases can be difficult to distinguish with some techniques.

At neutral pH, the zwitterionic DPPC headgroup is polar but neutral. Dipalmitoylphosphatidylglycerol (DPPG) differs from DPPC only in the substitution of a glycerol moiety for choline in the headgroup. At neutral pH, the DPPG headgroup carries a negative charge. At ambient pressure and in the absence of divalent cations such as calcium, the phase behaviour of DPPG is nearly identical to that of DPPC suggesting that the main liquid crystal to gel bilayer transition in these systems is more sensitive to interchain interactions than to the effects of headgroup charge. Differences between interactions involving the zwitterionic phosphocholine (PC) headgroup and the anionic phosphoglycerol (PG) headgroup do, however, affect bilayer properties in other ways. For example, Pabst et al. (2007) recently reported that the chain lengths for which disaturated lipids display a propensity to interdigitate are smaller for PGs than for PCs.

In this study, we have used ^{2}H-NMR spectral lineshapes and quadrupole echo decay times to compare the responses of chain-perdeuterated DPPC (DPPC-d_{62}) and chain-perdeuterated DPPG (DPPG-d_{62}) bilayers to pressures up to 196 MPa.

Materials and methods

Sample preparation

DPPC-d_{62} and DPPG-d_{62} were purchased from Avanti Polar Lipids (Birmingham, AL) and used without further purification. Samples were prepared by dissolving 25–30 mg of dry lipid powder in ethanol. The solution was then placed in a round-bottom flask from which the solvent was removed by heating to 40°C on a rotary evaporator. The sample was then maintained under vacuum for 12 h to remove residual solvent. The dry lipid was hydrated and removed from the wall of the flask by adding ~200 µl of 0.1 M phosphate buffer (pH 6.9–7.0) to the flask and then rotating it while holding the temperature at ~45°C. Samples were then spun briefly in a benchtop centrifuge to facilitate removal of excess buffer after which they were sealed into a flexible capsule formed by heat-sealing the ends of a short segment cut from a disposable polyethylene pipette.

Deuterium NMR

Wideline deuterium NMR observations were performed using a locally-constructed spectrometer and a 3.55 T superconducting solenoid (Nalorac Cryogenics, CA) in conjunction with variable-pressure wide-line NMR probe (Bonev and Morrow 1997a). The sample capsule and coil were inserted into a beryllium-copper cell that could be pressurized with hydraulic oil (AW ISO grade32). Pressures were measured using a Bourdon tube gauge that was previously calibrated against a dead-weight gauge.

Sample temperatures were controlled to ±0.1°C using a microprocessor-based PID controller in conjunction with a thermocouple sensor embedded in the wall of the pressure cell. Samples were allowed to equilibrate at each temperature for at least 30 min before the start of data acquisition. Spectra were obtained using a quadrupole echo pulse sequence (Davis et al. 1976) with a $\pi/2$ pulse length of 3.5 µs and pulse separations of 35–40 µs. Each spectrum was obtained by averaging 4,000–8,000 transients using quadrature detection with repetition times of 0.5–0.6 s. Oversampling (Prosser et al. 1991) was used to obtain effective dwell times of 4 µs for liquid crystalline samples and 2 µs for ordered phase samples. To facilitate first moment determination, spectra were symmetrized by phase correcting the free induction decay and then zeroing the imaginary channel before Fourier transforming. For echo decay measurements, echo amplitudes were measured with typical pulse separations of 35, 75, 100, 150, 200, 300 and 400 µs for samples with longer echo decay times and 35, 50, 75, 100, 150, 200, and 300 µs for samples with shorter

echo decay times. Average echo decay times were obtained by plotting the logarithm of the echo amplitude versus twice the pulse separation and inverting the slope of the initial decay.

Results and discussion

Figure 1 shows deuterium NMR spectra for DPPC-d_{62} and DPPG-d_{62} bilayers at ambient pressure, 85 and 196 MPa. Spectra were collected from high to low temperature. Figure 2 shows the temperature dependence of first moments, M_1, for these spectra where

$$M_1 = \frac{\int_0^\infty \omega f(\omega)\, d\omega}{\int_0^\infty f(\omega)\, d\omega} \quad (1)$$

and the intensity of a spectrum is represented by $f(\omega)$.

For ambient pressure and 85 MPa, the high temperature spectra for both lipids indicate a liquid crystalline (L_α) bilayer phase. These spectra are superpositions of doublets reflecting axially symmetric molecular reorientation about the bilayer normal on a timescale shorter than $\sim 10^{-5}$ s, the characteristic time for acquisition of the free induction decay for these experiments. The prominent edges of each doublet arise from molecules reorienting about bilayer normals that are perpendicular to the applied magnetic field. The splitting of a given doublet is proportional to the orientational order parameter, $S_{CD} = \langle 3\cos^2\theta - 1\rangle/2$ where θ is the angle between the CD bond and the axis about which the molecule is reorienting and the average is over motions of the CD bond that modulate the quadrupole interaction with correlation times that are short relative to $\sim 10^{-5}$ (Davis, 1983). The distribution of splittings in a given liquid crystalline spectrum reflects the dependence of orientational order on position along the deuterated hydrocarbon chain. The largest splittings correspond to the portion of the chain closest to the headgroup where motions are most constrained. For methylene segments near the headgroup end of the acyl chains, orientational order changes slowly with position along the chain and a plot of orientational order parameter versus position along the chain displays a plateau. Doublets with the smallest splittings correspond to deuterated methylene segments near the bilayer centre where chain reorientation is least constrained. The first spectral moment, M_1, is proportional to the average, taken over all chain deuterons, of the orientational order parameter in the axially symmetric phase and provides a useful indication of average chain order at lower temperatures where the spectral contributions from individual chain deuterons cannot be resolved.

At ambient pressure, both lipids display a sharp transition from the liquid crystalline phase (L_α) to a gel phase. For DPPC-d_{62}, the transition occurs between 37 and 36°C.

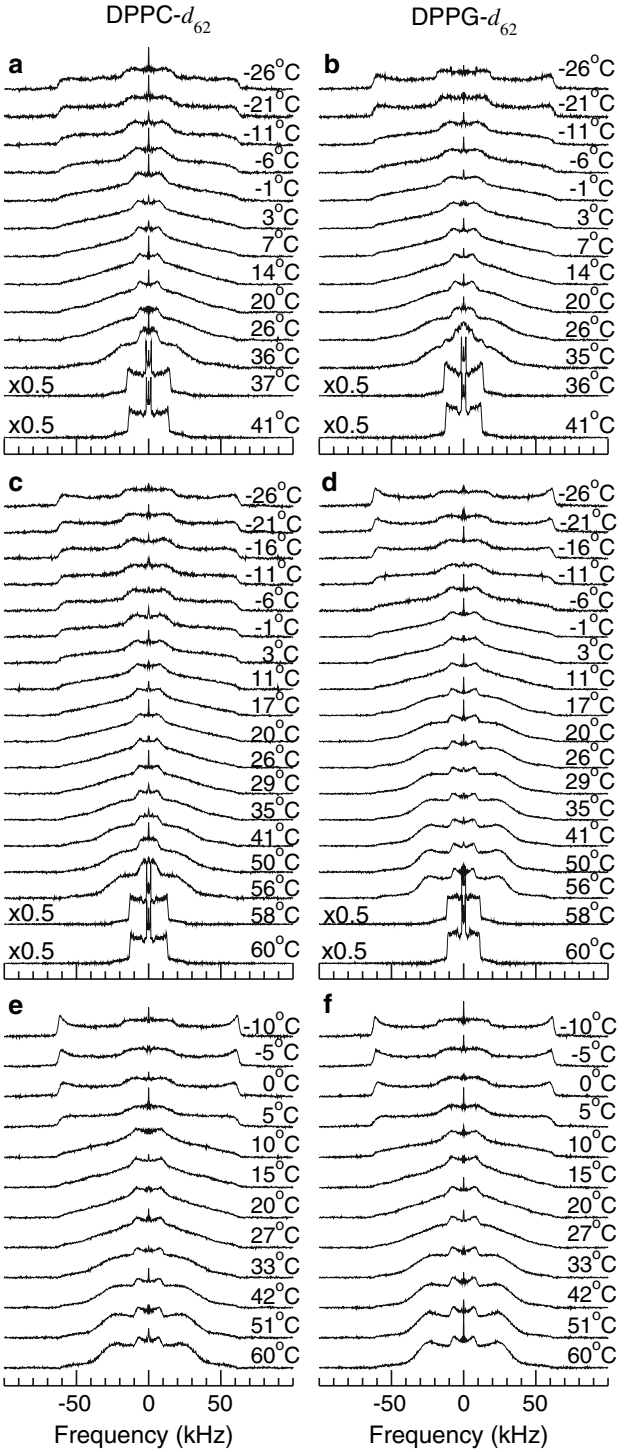

Fig. 1 ^{2}H NMR spectra at selected temperatures for **a** DPPC-d_{62} at ambient pressure, **b** DPPG-d_{62} at ambient pressure, **c** DPPC-d_{62} at 85 MPa, **d** DPPG-d_{62} at 85 MPa, **e** DPPC-d_{62} at 196 MPa, and **f** DPPG-d_{62} at 196 MPa

For DPPG-d_{62}, the transition is about 1°C lower. The gel phase spectra are characteristic of more ordered chains reorienting on a timescale longer than the characteristic deuterium NMR timescale. The ambient pressure M_1 data

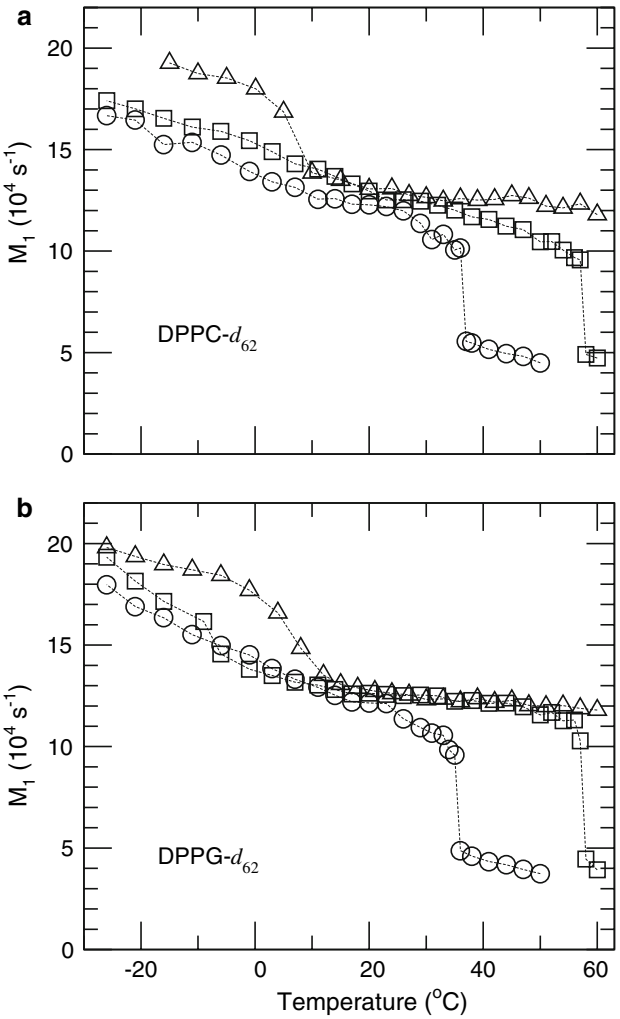

Fig. 2 Temperature dependence of the ^{2}H-NMR first spectral moment (M_1) for **a** DPPC-d_{62} and **b** DPPG-d_{62} bilayers at *open circles* ambient pressure, *open squares* 85 MPa, and *open triangles* 196 MPa

plotted in Fig. 2 show that the discontinuities in average chain order at the main ambient pressure transitions of the two lipid systems are effectively indistinguishable.

For DPPC-d_{62}, the phase immediately below the main transition is a rippled gel phase, $P_{\beta'}$. Between 29 and 26°C, there is a transition to a more planar gel phase, $L_{\beta'}$, in which molecules are tilted with respect to the bilayer normal (Janiak et al. 1976). Spectra in the $P_{\beta'}$ phase are characterized by sloping shoulders and a methyl component characterized by two slightly different splittings (Westerman et al. 1982; Davis 1983; Vist and Davis 1990). In the $L_{\beta'}$ phase, the intensity drops off more smoothly from the centre to the wings of the spectrum and the methyl feature is wider and less structured (Vist and Davis 1990). Near the $P_{\beta'} \rightarrow L_{\beta'}$ transition, the differences between the $P_{\beta'}$ and $L_{\beta'}$ spectra can be small. We will refer to a gel phase when no distinction is intended.

As temperature is lowered further at ambient temperature, the spectra from both lipid bilayer samples display increasing intensity near ±63 kHz. This reflects the gradual transformation to a phase in which the hydrocarbon chains are effectively immobilized on the deuterium NMR timescale so that the effective axis of symmetry for the quadrupole interaction of each deuteron lies along the carbon-deuterium bond. The resulting spectrum reflects the full quadrupole interaction and is typical of the subgel or lamellar crystalline (L_C) phase (Davis 1979; Chen et al. 1980; Nagle and Wilkinson 1982; Morrow et al. 1992). In this phase, fast rotation about the methyl group axis reduces the splitting for the methyl deuterons at the chain ends by about a third and accounts for the prominent feature between ±18 kHz. The lipid chain reorganization associated with the gel to L_C transition is typically very slow (Nagle and Wilkinson 1982). Even with equilibration times of an hour or more before acquisition of the spectrum at a given temperature, this transition, as reflected by the ambient pressure spectra in Fig. 1, occurs over a broad temperature range starting near −1°C and extending to below −11°C for both lipids.

At 85 MPa, the spectra for both lipid systems reflect transitions from the L_α phase to ordered phases at effectively identical temperatures of 57°C. For DPPC-d_{62}, the ordered phase below this transition appears to be the gel ($P_{\beta'}$) phase seen at ambient pressure. For DPPG-d_{62}, however, the spectra just below the transition reflect a bilayer phase that is more ordered than the corresponding $P_{\beta'}$ phase of DPPC-d_{62}. The M_1 data plotted in Fig. 2 for 85 MPa shows that the discontinuity in average chain order at the main transition for that pressure is larger for DPPG-d_{62} than for DPPC-d_{62} suggesting that the main transition at this pressure is sensitive to the difference in headgroup charge of these two lipids.

The DPPG-d_{62} spectrum just below the transition at 85 MPa (Fig. 1d) displays prominent shoulders near ±30 kHz. These are more pronounced than in the $P_{\beta'}$ spectrum and the splitting of the methyl feature is larger than in the $P_{\beta'}$ spectrum. A carbon-deuterium bond undergoing axially symmetric reorientation about an axis with the angle between the bond and that axis constrained to be close to 90° would give rise to a Pake doublet with the prominent edges split by about 66 kHz. The DPPG-d_{62} spectrum just below the 85 MPa transition in Fig. 1d thus reflects a bilayer state in which chains are highly ordered and reorienting about the bilayer normal but with a correlation time that is too long for the reorientation to be axially symmetric on the characteristic time scale ($\sim 10^{-5}$ s) of the deuterium spectral acquisition time. The chain orientational order reflected by this spectrum is higher than in the $P_{\beta'}$ phase. For DPPC-d_{62}, similar spectra were observed (Driscoll et al. 1991b; Bonev and Morrow 1998) at

pressures and temperatures for which neutron diffraction studies (Braganza and Worcester 1986a) previously indicated the interdigitated gel phase ($L_{\beta I}$) of DPPC. The higher orientational order reflected by the spectrum with prominent shoulders near ±30 kHz is consistent with the motional constraints expected near the centre of an interdigitated gel bilayer and we have assumed that identification in what follows. It should be noted, however, that this spectral shape cannot be exclusively associated with an interdigitated phase and that similar shapes have been reported for other bilayer phases in which with high orientational order reorient about the bilayer normal. For example, the spectral shape identified here as indicative of an interdigitated phase is superficially similar to spectra reported for DPPC-d_{62} bilayers containing 5–6 mole percent cholesterol at 36°C (Vist and Davis 1990). At that cholesterol concentration, the DPPC-d_{62} acyl chains are more highly ordered than the normal gel but their reorientation is less axially symmetric than is observed in the cholesterol-rich liquid-ordered phase.

For DPPC-d_{62}, the 85 MPa spectra in Fig. 1c evolve from being characteristic of $P_{\beta'}$ at 41°C to being more characteristic of $L_{\beta'}$ at 26°C but it is difficult to identify a transition temperature from either the spectra or the first moments. For DPPG-d_{62}, the spectra at 85 MPa (Fig. 1d) gradually change from being characteristic of the interdigitated gel, $L_{\beta I}$, just below to the main transition to being more characteristic of $L_{\beta'}$ at 11°C but again it is difficult to identify a transition temperature from either the spectra or the first moments (Fig. 2b).

As temperature is reduced further, the 85 MPa spectra of both DPPC-d_{62} (Fig. 1c) and DPPG-d_{62} (Fig. 1d) again develop significant intensity near ±63 kHz indicating onset of the transition into the L_C phase. For both DPPC-d_{62} and DPPG-d_{62}, growth of the prominent spectral edges near ±63 kHz is again spread over a range of more than 10°C. For DPPC-d_{62}, comparison of the spectra in Fig. 1a and c and comparison of the ambient pressure and 85 MPa first moments in Fig. 2a suggests that the broad transition into the L_C phase at 85 MPa is shifted upwards by about 10°C relative to the ambient pressure transition. For DPPG-d_{62}, there is less shift of this transition between ambient pressure and 85 MPa.

At 85 MPa, the behaviours of DPPC-d_{62} and DPPG-d_{62} differ in the sequence of gel phases between the main transition and the onset of the chain immobilization in the L_C phase. For DPPC-d_{62} at 85 MPa (Fig. 1c), the sequence of phases observed on cooling from above the main transition is the same as at ambient pressure. The transition from liquid crystalline (L_α) to gel ($P_{\beta'}$) occurs between 58 and 57°C and a transition from gel ($L_{\beta'}$) to lamellar crystalline (L_C) begins near 11°C and continues to below −1°C. The $P_{\beta'}$–$L_{\beta'}$ transition occurs between 40° and 30° but is difficult to localize more precisely from inspection of the gel phase spectra.

For DPPG-d_{62} at 85 MPa (Fig. 1d), the spectrum changes gradually from being characteristic of the interdigitated gel phase ($L_{\beta I}$) to characteristic of the chain-immobilized (L_C) phase as the sample is cooled from below the main transition. The shoulders near ±30 kHz persist to at least as low as 29°C and the edge at ±63 kHz characteristic of the L_C phase develops significantly between −1 and −11°C. At 85 MPa, the spectra for DPPG-d_{62} at 17°C and for DPPC-d_{62} at 11°C are very similar suggesting that DPPG-d_{62} changes from the interdigitated $L_{\beta I}$ phase back to a normal gel phase before ordering into the subgel or L_C phase on further cooling. For DPPC, which interdigitates at higher pressure, most reported phase diagrams show a transition from the interdigitated gel phase to a phase that has variously been identified as simply gel (Braganza and Worcester 1986a; Winter and Pilgrim 1989), $L_{\beta'}$ (Ichimori et al. 1998), or the higher-pressure GIII phase (Wong et al. 1988; Dirscoll et al. 1991b). The sequence of phases encountered on cooling DPPG-d_{62} at 85 MPa from the L_α thus appear to be qualitatively similar to those encountered on cooling DPPC at higher pressure.

At 196 MPa, the behaviours of the two lipids are again similar. At 60°C, the highest temperature for which spectra were obtained, both lipids display spectra with prominent shoulders near ±30 kHz. DPPC is known to interdigitate at this temperature and pressure (Braganza and Worcester 1986a) and the 60°C spectra of both lipids in Fig. 1e and f are similar to those previously reported for DPPC-d_{62} under conditions of temperature and pressure consistent with interdigitation (Driscoll et al. 1991b; Bonev and Morrow 1997b). This comparison confirms the identification of these spectra as indicative of interdigitation and indicates that both lipids are in interdigitated ($L_{\beta I}$) gel phases at 196 MPa and 60°C.

Spectral indications of interdigitaiton persist down to about 30°C for both lipids (Fig. 1e and f). For both lipids, onset of the transition into the L_C phase, as indicated by the development of significant intensity near ±63 kHz, occurs between 10 and 4°C. Both lipids appear to pass through a non-interdigitated gel phase between the $L_{\beta I}$ and L_C phases. As noted above, the phase seen on cooling DPPC, at high pressure, from the interdigitated phase into a non-interdigitated gel phase has been identified as either $L_{\beta'}$ or GIII. Differences in the spectral shapes for these phases are small (Driscoll et al. 1991b; Bonev and Morrow 1997b).

The phase behaviour described above is also reflected by the temperature dependence of quadrupole echo decay times for the two lipid samples at different pressures. In a quadrupole echo experiment, dephasing of the precessing deuteron magnetization following an initial pulse is reversed by a second pulse at time τ and an echo is formed

at time 2τ. The amplitude of the echo reflects the extent to which the orientation-dependent quadrupole interaction has been left unchanged by molecular motions during this time. The rate with which the signal from a given deuteron decays with increasing 2τ is a superposition of contributions, R_i, from all motions, indexed by i, that modulate the quadrupole interaction for that carbon-deuterium bond. The contribution to the echo from a given deuteron then decays with a characteristic time $T_{2i}^{qe} = \left(\sum_i R_i\right)^{-1}$.

A particular motion, i, can be characterized by its correlation time, τ_{ci}, and the second moment of that part of the quadrupole interaction modulated by that motion, ΔM_{2i}. A motion can be classified as fast or slow based on comparison τ_{ci} with $(\Delta M_{2i})^{-1/2}$ (Bloom and Sternin 1987). For a particular fast motion, the contribution to echo decay rate, R_i, is proportional to $\Delta M_{2i}\tau_{ci}$ (Abragam 1961; Bloom and Sternin 1987). For slow reorientations, $R_i \propto \tau_{ci}^{-1}$ (Pauls et al. 1985). Echo decay in the L_α phase is affected by slow motions, like bilayer undulations, and faster motions like reorientation about the bilayer normal (Bloom and Sternin 1987; Bloom and Evans 1991; Stohrer et al. 1991).

At the main transition from L_α to a more ordered gel phase, the correlation times for all motions increase. A motion that is slow in the liquid crystalline phase will also be slow below the transition. Its contribution to the echo decay rate will be proportional to τ_{ci}^{-1} above and below the transition and will thus decrease on cooling through the transition. If a particular motion is fast in the liquid crystalline phase, so that $R_i \propto \tau_{ci}$, its contribution to the echo decay rate will generally increase at the transition. Below the transition, though, there are two possibilities for how such a motion will contribute to echo decay. If the increase in correlation time at the transition moves the motion from the fast to the slow motion regime, its contributions to echo decay will decrease as temperature is further reduced. The increase in echo decay time normally observed with decreasing temperature just below the liquid crystal to gel transition likely reflects the slowing of motions such as molecular reorientation about and with respect to the bilayer normal (Kilfoil and Morrow 1998). On the other hand, internal molecular motions may remain in the fast motion regime below the transition. In this case, the contribution to echo decay rate will continue to increase as temperature is reduced and the total echo decay rate will pass through a minimum at a temperature below which the remaining fast internal motions will dominate.

Figure 3 shows echo decay times corresponding to the ambient pressure, 85 and 196 MPa series of DPPC-d_{62} and DPPG-d_{62} spectra in Fig. 1. At ambient pressure, the echo decay times for DPPC-d_{62} (Fig. 3a) and DPPG-d_{62} (Fig. 3b) depend similarly on temperature. This temperature dependence is typical of saturated-chain lipid bilayers at ambient pressure (Simatos et al. 1990; Weisz et al. 1992;

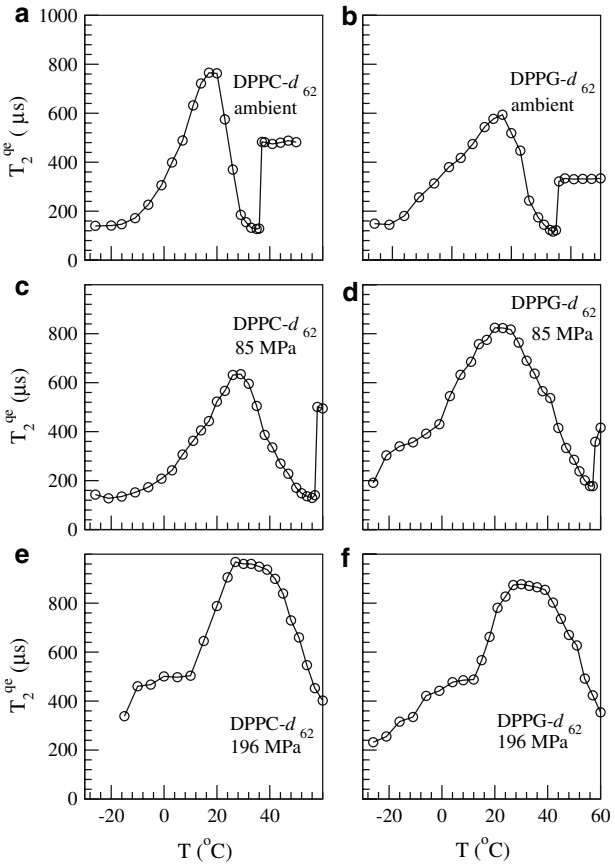

Fig. 3 Temperature dependence of the quadrupole echo decay time for **a** DPPC-d_{62} at ambient pressure, **b** DPPG-d_{62} at ambient pressure, **c** DPPC-d_{62} at 85 MPa, **d** DPPG-d_{62} at 85 MPa, **e** DPPC-d_{62} at 196 MPa, and **f** DPPG-d_{62} at 196 MPa

Kilfoil and Morrow 1998; Morrow et al. 2004). In the liquid crystalline phase, the contributions to the echo decay rate from slow motions decreases as the temperature is reduced while the contributions from faster molecular motions, such as reorientation about the bilayer normal, increase with decreasing temperature. The resulting superposition is roughly independent of temperature in the liquid crystalline phase. At the transition to the gel phase, the contributions from faster molecular motions increase discontinuously and the observed echo decay rate drops sharply. Below about 20°C, the contributions to the echo decay rate from the fast internal motions become significant and the echo decay times pass through a maximum and begin to drop with decreasing temperature.

At 85 MPa, the behaviours of the quadrupole echo decay times for the two lipids are different. For DPPC-d_{62} (Fig. 3c), the behaviour at 85 MPa is qualitatively similar to that seen at ambient pressure except for a shift in main transition temperature and an increase in the width of the peak in echo decay time below the transition. The spreading of this peak across a wider temperature range implies that the corresponding minimum in echo decay rate

is broader and shallower and thus that the freezing out of both fast and slow motions below the transition occurs more slowly with decreasing temperature than at ambient temperature.

For DPPG-d_{62} at 85 MPa (Fig. 3d), the maximum echo decay time is higher and occurs about 10° lower than for DPPC-d_{62}. One particularly striking difference is the reduced dependence of the DPPG-d_{62} echo decay time on temperature near the onset of the transition to the L_C phase as the temperature is lowered. The result is a plateau-like feature in the echo decay time curve between 0 and −10°C.

The increase in echo decay time on cooling of the sample from just below the main transition temperature to the echo decay time peak, near 20°C for DPPG-d_{62} at 85 MPa, reflects freezing out of motions that are in the slow regime just below the main transition. For temperatures below the echo decay time peak and, particularly, at the temperature of the plateau in Fig. 3d, echo decay is dominated by residual fast internal molecular motions, such as trans-gauche isomerization, for which $R_i \propto \tau_{ci}$. The shape of the echo decay time curve between 20 and −20°C in Fig. 3d thus suggests that for at least one fast motion, $\Delta M_{2i}\tau_{ci}$ increases more quickly from 20°C to 0°C (between $L_{\beta I}$ and the onset of the L_C phase transformation) than it does from 0 to −20°C (during development of L_C phase order).

Comparison of Fig. 3c and d shows that, at 85 MPa, the peak in the echo decay time curve for DPPG-d_{62} is higher and occurs at lower temperature than for DPPC-d_{62}. This indicates that the temperature at which the fast motions begin to dominate echo decay at 85 MPa is slightly lower for DPPG-d_{62} than for DPPC-d_{62}. This also suggests that, for any temperature below the main transition at 85 MPa, $\Delta M_{2i}\tau_{ci}$ for a given DPPG-d_{62} fast motion is smaller than the contribution to echo decay rate from a corresponding DPPC-d_{62} fast motion.

At 196 MPa, the plots of quadrupole echo decay time versus temperature for DPPC-d_{62} (Fig. 3e) and DPPG-d_{62} (Fig. 3f) are very similar and, except for the shift expected due to the pressure dependence of the main phase transition, also very similar to the plot for DPPG-d_{62} at 85 MPa (Fig. 3d). In particular, these plots display a reduced sensitivity of quadrupole echo decay time to temperature over the range for which the spectra develop significant intensity near ±63 kHz. This indicates that the characteristic shape of the echo decay time curves in Fig. 3d, e, and f reflects the sequence of high pressure phases going from $L_{\beta I}$ to L_C and that the observed shape is not specific to one of the two lipid species studied.

A more detailed understanding of the difference between the ambient pressure and high pressure behaviours of ordered phase quadrupole echo decay time would require additional experiments, perhaps with specifically-deuterated lipids. However, comparison of Fig. 3a, b and c with Fig. 3d, e and f does suggest that the phase that occurs on cooling from the $L_{\beta I}$ phase to the L_C phase at high pressure, for both lipids, can be distinguished from the $L_{\beta'}$ phase that occurs on cooling from the $P_{\beta'}$ phase to the L_C phase at ambient pressure. This would be consistent with reports of a distinct phase, labelled GIII, in this portion of the phase diagram (Wong et al. 1988; Driscoll et al. 1991b).

Based on both spectra and quadrupole echo decay time observations, DPPC-d_{62} and DPPG-d_{62} behave similarly at ambient pressure. Their behaviours at 196 MPa are also similar and distinct from their ambient pressure behaviours. At 85 MPa, the behaviour of DPPC-d_{62} is more characteristic of its ambient pressure behaviour and the behaviour of DPPG-d_{62} is more characteristic of its higher pressure behaviour.

One of the most striking of these observations is that the interdigitated gel phase of DPPG-d_{62} appears to be stable at lower pressure than the corresponding phase of DPPC-d_{62}. This presumably reflects differences between the two lipids having to do with interactions at their membrane surfaces. In order to more fully characterize this difference, spectra for both systems were collected while varying pressure at a series of fixed temperatures separated by 5° and ranging from 5 to 60°C.

Figure 4 shows DPPC-d_{62} and DPPG-d_{62} spectra at selected pressures for 55 and 40°C. At 55°C, DPPC-d_{62} (Fig. 4a) undergoes a transition from L_α to gel ($P_{\beta'}$) as pressure is increased from 83.1 to 97.9 MPa. As pressure is raised beyond 100 MPa, the spectral shape changes gradually to that of the interdigitated $L_{\beta I}$ phase. For DPPG-d_{62} at 55°C, the observed transition is directly from L_α to $L_{\beta I}$. At 40°C, DPPC-d_{62} (Fig. 4c) again transforms from L_α to $P_{\beta'}$ and then to $L_{\beta I}$ as pressure is increased. The L_α to $P_{\beta'}$ transition is at lower pressure than for 55°C. DPPG-d_{62} at 40°C (Fig. 4d) also passes through the $P_{\beta'}$ phase before transforming to the $L_{\beta I}$ phase as pressure is raised.

Figure 5 shows DPPC-d_{62} and DPPG-d_{62} spectra at selected pressures for 35, 20 and 5°C. At 35°C, both lipids are in the $P_{\beta'}$ phase at ambient pressure. The DPPC-d_{62} spectra (Fig. 5a) gradually change as pressure is raised but remain largely characteristic of $P_{\beta'}$ at 165 MPa. The DPPG-d_{62} spectra (Fig. 5b) develop shoulders characteristic of the $L_{\beta I}$ phase for pressures above 55.9 MPa. At 20°C, both lipids (Fig. 5c, d) are in a gel phase at ambient pressure. The spectra become increasingly characteristic of $L_{\beta'}$ as pressure is raised. The development of intensity near ±63 kHz suggests that both lipids are close to the transition into L_C at high pressure. At 5°C, the spectra of both lipids (Fig. 5e, f) have some intensity near ±63 kHz at ambient pressure and the spectra become increasingly characteristic of the L_C phase as pressure is raised.

In order to summarize these observations, each spectrum collected in this study was inspected and classified as

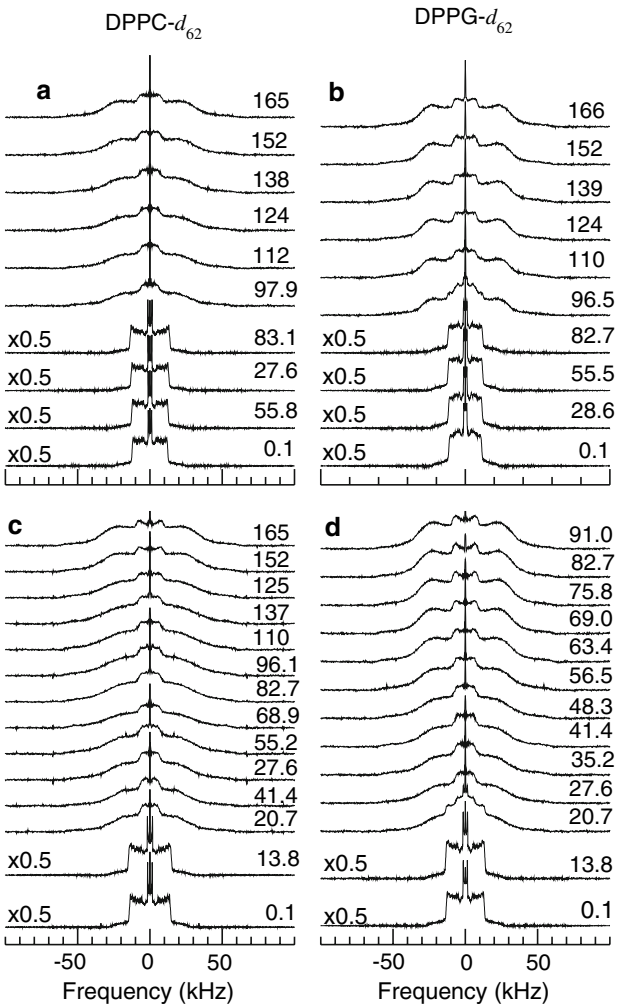

Fig. 4 ^{2}H NMR spectra at selected pressures for **a** DPPC-d_{62} at 55°C, **b** DPPG-d_{62} at 55°C, **c** DPPC-d_{62} at 40°C, and **d** DPPG-d_{62} at 40°C

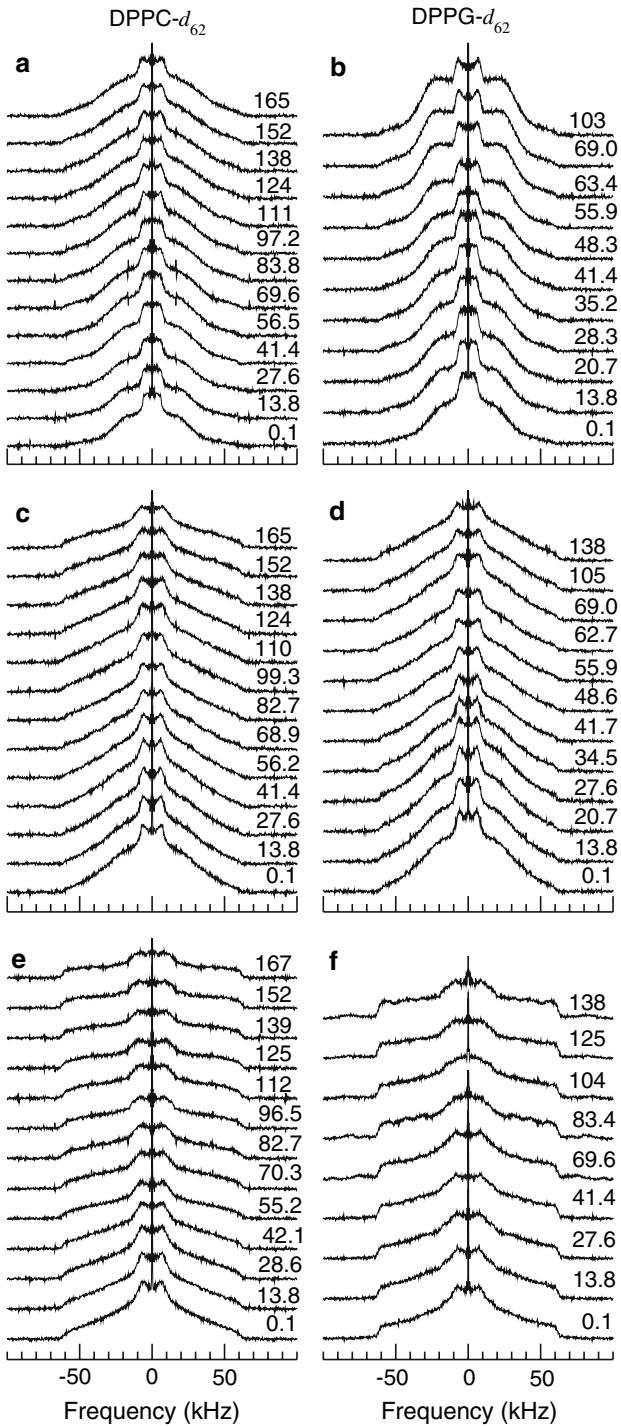

Fig. 5 ^{2}H NMR spectra at selected pressures for **a** DPPC-d_{62} at 35°C, **b** DPPG-d_{62} at 35°C, **c** DPPC-d_{62} at 20°C, **d** DPPG-d_{62} at 20°C, **e** DPPC-d_{62} at 5°C, and **f** DPPG-d_{62} at 5°C

characteristic of L_α, L_C, $L_{\beta I}$, or gel. While it was possible to distinguish $P_{\beta'}$, $L_{\beta'}$, and perhaps even GIII near extremes of their ranges, it was difficult to reliably identify transitions between these phases on the basis of spectral differences and they were classified collectively as gel. The spectral changes on moving from $L_{\beta I}$ to gel and from gel to L_C were also gradual but usually could be localized to within a few spectra in a given isothermal or isobaric series. The results are summarized as pressure-temperature diagrams in Fig. 6. The isobaric and isothermal spectral series gave consistent results at ambient pressure. At high pressure, the gel to L_C transitions indicated by the isobaric series occurred at lower temperatures than were inferred from the isothermal series. Reorganization of the lipid chains into the subgel or L_C phase is known to proceed very slowly (Nagle and Wilkinson 1982; Morrow et al. 1992) and discrepancies between isothermal and isobaric observations of this transition are not surprising.

The pressure-temperature diagrams in Fig. 6 display some interesting similarities and differences. The ambient pressure phase behaviours of DPPC-d_{62} and DPPG-d_{62} are strikingly similar. The boundaries of the L_α regions on the two diagrams are also very similar. There may be a slight difference in the L_C boundaries at high pressure but this

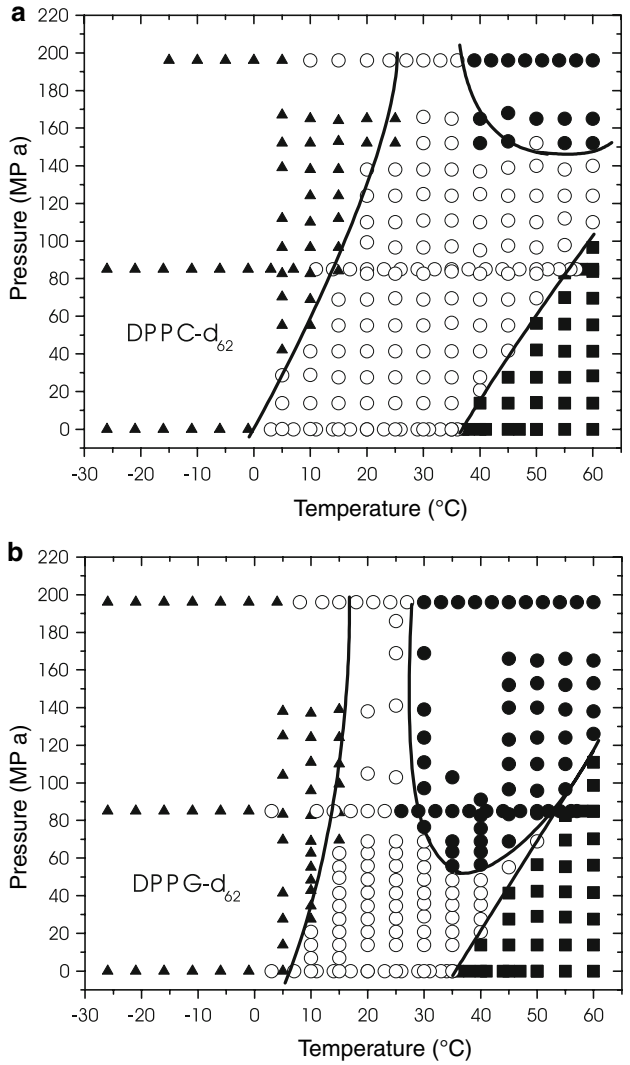

Fig. 6 Pressure–temperature phase diagrams for **a** DPPC-d_{62} and **b** DPPG-d_{62} bilayers obtained by inspection of ^{2}H NMR spectral shapes. Phases indicated are *filled squares* L_α, *open circles* gel which includes $P_{\beta'}$, $L_{\beta'}$, and GIII without distinction, *filled triangles* L_C, and *filled circles* $L_{\beta I}$. Except for the L_α boundary, uncertainties in boundary positions are of the order of the spacing between adjacent symbols. *Solid lines* are visual aids only

may also reflect the kinetics of the gel to L_C transition. There was little difference between the isobaric series of the two lipids at 196 MPa.

The obvious difference between the two pressure-temperature diagrams is the persistence of the DPPG-d_{62} interdigitated gel phase to significantly lower pressures than for DPPC-d_{62}. It has recently been reported that distearoyl phosphatidylglycerol (DSPG) can exist in an $L_{\beta I}$ phase under conditions for which the corresponding phosphocholine (DSPC) is not interdigitated (Pabst et al. 2007). In both cases, the higher propensity for interdigitation on the part of a disaturated PG, relative to the corresponding PC under comparable conditions, presumably reflects differences in the headgroup charge and shape of the two otherwise identical lipid species. Pabst et al. (2007) suggest that one difference lies in the ability of the PC and PG lipids to accommodate changes in headgroup tilt. The observation, here, that DPPC-d_{62} and DPPG-d_{62} behave similarly at high and low pressure but respond differently to intermediate pressure underlines how sensitive bilayer phase behaviour is to the balance between headgroup and hydrocarbon chain interactions.

Acknowledgments This research was supported by grants to MRM from the Natural Science and Engineering Research Council of Canada.

References

Abragam A (1961) The principles of nuclear magnetism. Oxford University Press, London

Bloom M, Evans E (1991) Observation of surface undulations on the mesoscopic length scale by NMR. In: Peliti L (ed) Biologically Inspired Physics. Plenum Press, New York, pp 137–147

Bloom M, Sternin E (1987) Transverse nuclear spin relaxation in phospholipids bilayer membranes. Biochemistry 26:2101–2105

Bonev BB, Morrow MR (1997a) Simple probe for variable pressure deuterium nuclear magnetic resonance studies of soft materials. Rev Sci Instrum 68:1827–1830

Bonev BB, Morrow MR (1997b) Effect of pressure on the dimyristoylphosphatidyl-choline bilayer main transition. Phys Rev E 55:5825–5833

Bonev BB, Morrow MR (1998) ^{2}H NMR studies of dipalmitoylphosphatidylcholine and dipalmitoylphosphatidylcholine-cholesterol bilayers at high pressure. Can J Chem 76:1512–1519

Böttner M, Ceh D, Jacobs U, Winter R (1994) High pressure volumetric measurements on phospholipids bilayers. Z Phys Chem 184:205–218

Braganza LF, Worcester DL (1986a) Hydrostatic pressure induces hydrocarbon chain interdigitation in single-component phospholipids bilayers. Biochemistry 25:2591–2596

Braganza LF, Worcester DL (1986b) Structural changes in lipid bilayers and biological membranes caused by hydrostatic pressure. Biochemistry 25:7484–7488

Chen SC, Sturtevant JM, Gaffney BJ (1980) Scanning calorimetric evidence for a third phase transition in phosphatidylcholine bilayers. Proc Natl Acad Sci USA 77:5060–5063

Czeslik C, Reis O, Winter R, Rapp G (1998) Effect of high pressure on the structure of dipalmitoylphosphatidylcholine bilayer membranes: a synchrotron-X-ray diffraction and FT-IR spectroscopy study using the diamond anvil technique. Chem Phys Lipids 91:135–144

Davis JH (1979) Deuterium magnetic resonance study of the gel and liquid crystalline phases of dipalmitoyl phosphatidylcholine. Biophys J 27:339–358

Davis JH (1983) The description of membrane lipid conformation, order and dynamics by ^{2}H-NMR. Biochim Biophys Acta 737:117–171

Davis JH, Jeffrey KR, Bloom M, Valic MI, Higgs TP (1976) Quadrupole echo deuteron magnetic resonance spectroscopy in ordered hydrocarbon chains. Chem Phys Lett 42:390–394

Driscoll DA, Samarasinghe S, Adamy S, Jonas J, Jonas A (1991a) Pressure effects on dipalmitoylphosphatidylcholine bilayers measured by ^{2}H nuclear magnetic resonance. Biochemistry 30:3322–3327

Driscoll DA, Jonas J, Jonas A (1991b) High pressure ^{2}H nuclear magnetic resonance study of the gel phases of dipalmitoylphosphatidylcholine. Chem Phys Lipids 58:97–104

Ichimori H, Hata T, Matsuki H, Kaneshina S (1998) Barotropic phase transitions and pressure-induced interdigitation on bilayer membranes of phospholipids with varying acyl chain lengths. Biochim Biophys Acta 1414:165–174

Janiak MJ, Small DM, Shipley GG (1976) Nature of the thermal pretransition of synthetic phospholipids: dimyristoyl- and dipalmitoyllecithin. Biochemistry 15:4575–4580

Kaneshina S, Tamura K, Kawakami H, Matsuki H (1992) Effects of pressure and ethanol on the phase behaviour of dipalmitoylphosphatidylcholine multilamellar vesicles. Chem Lett 1963–1966

Kilfoil ML, Morrow MR (1998) Slow motions in bilayers containing anionic phospholipids. Physica A 261:82–94

Maruyama S, Hata T, Matsuki H, Kaneshina S (1997) Effects of pressure and local anesthetic tetracaine on dipalmitoylphosphatidylcholine bilayers. Biochim Biophys Acta 1325:272–280

Morrow MR, Whitehead JP, Lu D (1992) Chain-length dependence of lipid bilayer properties near the liquid crystal to gel phase transition. Biophys J 63:18–27

Morrow MR, Stewart J, Taneva S, Dico A, Keough KMW (2004) Perturbation of DPPC bilayers by high concentrations of pulmonary surfactant protein SP-B. Eur Biophys J 33:285–290

Nagle JF, Wilkinson DA (1982) Dilatometric studies of the subtransition in dipalmitoylphosphatidylcholine. Biochemistry 21:3817–3821

Pabst G, Danner S, Karmakar S, Deutsch G, Raghunathan VA (2007) On the propensity of phosphatidylglycerols to form interdigitated phases. Biophys J 93:513–525

Pauls K, MacKay A, Söderman O, Bloom M, Tangea A, Hodges R (1985) Dynamic properties of the backbone of an integral membrane polypeptide measured by ^{2}H-NMR. Eur Biophys J 12:1–11

Prosser RS, Davis JH, MacKay AL (1991) ^{2}H nuclear magnetic resonance of the gramicidin A backbone in a phospholipid bilayer. Biochemistry 30:4687–4696

Simatos GA, Forward KB, Morrow MR, Keough KMW (1990) Interaction between perdeuterated dimyristoylphosphatidylcholine and low molecular weight pulmonary surfactant protein SP-C. Biochemistry 29:5807–5814

Stohrer J, Gröbner G, Reimer D, Weisz K, Mayer C, Kothe G (1991) Collective lipid motions in bilayer membranes studied by transverse deuteron spin relaxation. J. Chem Phys 95:672–678

Vist MR, Davis JH (1990) Phase equilibria of cholesterol/dipalmitoylphosphatidylcholine mixtures: ^{2}H nuclear magnetic resonance and differential scanning calorimetry. Biochemistry 29:451–464

Weisz K, Gröbner G, Mayer C, Stohrer J, Kothe G (1992) Deuteron nuclear magnetic resonance study of the dynamic organization of phospholipids/cholesterol bilayer membranes: Molecular properties and viscoelastic behaviour. Biochemistry 31:1100–1112

Westerman PW, Vaz MJ, Strenk LM, Doane JW (1982) Phase transitions in phosphatidylcholine multibilayers. Proc Natl Acad Sci USA 79:2890–2894

Winter R, Pilgrim W-C (1989) A SANS study of high pressure phase transitions in model biomembranes. Ber Bunsenges Phys Chem 93:708–717

Wong PTT, Siminovitch DJ, Mantsch HH (1988) Structure and properties of model membranes: new knowledge from high-pressure vibrational spectroscopy. Biochim Biophys Acta 947:139–171